ON EXPERIMENTAL-ANALYTICAL EVALUATION OF PASSENGER CAR RIDE QUALITY SUBJECT TO ENGINE AND ROAD DISTURBANCES

Neda Nickmehr, Jan Åslund, Lars Nielsen, and Kristoffer Lundahl

Division of Vehicular Systems, Dept. of Electrical Engineering, Linköping University, 581 83 Linökping, Sweden,
e-mail: neda.nickmehr@isy.liu.se

A straightforward approach is presented to investigate the ride dynamic system for a typical rear-drive passenger car. The procedure is based on introducing two main ride excitation sources, i.e., engine/driveline and road inputs, which reduce passengers' comfort. The measured engine fluctuating torques are applied on the coupled model of the driveline and the suspension, to obtain the vehicle body longitudinal vibration. Further, the body vertical response to an average road roughness, is found by employing the quarter-car model. Through the frequency analysis done in this paper, it is shown that we can fastly determine the transfer functions of the systems and also their forced responses at the desired positions, without guessing any initial conditions for the states. The results illustrate that the high frequency inputs, from the engine, are appropriately damped by the current suspension. Hence, the associated vehicle body longitudinal acceleration meets the International Standard Organization (ISO) criteria. This is not the case for the low frequency disturbances, from the road surface irregularities, where the vehicle body vertical acceleration is above the ISO criteria.

1. Introduction

Over the last two decades, ride quality has received a great attention in automotive industry among the manufacturers. Consequently, more research efforts, in vehicle design area, have been devoted to this subject. Ride quality is an important topic in vehicle refinement, which aims to study and control the levels of noise and vibration so as to achieve more comfortable, more silent, and safer cars according to customers' demand [1].

There are two different frequency regions in the vehicle noise and vibration spectrum that are important. First, the ride interval which includes the frequencies between $1 - 100$ Hz and, second, the noise interval which addresses the frequency range $30 - 4000$ Hz. The ride frequency range is reported by the International Standard Organization (ISO) for evaluation of passenger comfort to the whole body vibration [2]. Ride dynamic system investigation is composed of three main parts. First, introduction of major excitation sources, namely, driveline/engine and road irregularities. Second, obtaining vehicle dynamic response subject to these excitations and, third, the human perspicacity.

The driveline is a lightly damped dynamic system, consisting of the inertia and the elastic elements. It is the most significant origin of the vehicles' noise and vibration. These vibrations are transferred to the chassis thereby attenuating the passenger comfort. Torsional frequencies of the driveline are excited by various numbers of resources such as engine disturbances and road roughness

inputs. The exciting inputs from the engine can be divided, specifically, in two categories. The first is sudden/discrete such as tip-in/tip-out maneuvers and throttle inputs. The second is continuous such as engine torque fluctuations that include gas and inertia torques [3].

A number of investigations have been devoted to the modeling of driveline torsional vibration [4, 5]. Farshidianfar *et al* provided a general lumped parameter model of the driveline and used MATLAB SIMULINK for vibration analysis subject to an impulse input without representing a separate model for the engine part [6]. The first natural frequency, i.e., driveline shuffle, was also identified by [6]. Rabeih developed a 14-degrees-of-freedom lumped parameter model, from the engine to the driving wheels, for torsional vibration of the driveline [7]. The damped natural frequencies of the system were found, in [7], using the eigenvalue method. Further, the responses of the driveline system, at different positions, were determined subject to the engine fluctuating torque by modal analysis and a Runge-kutta numerical technique. As opposed to [6], the work in [7] provides an independent lumped model for the engine substructure where the engine oscillatory torque was obtained analytically using the harmonic coefficients of the gas pressure [7]. The coupled torsional vibration of the driveline with the body longitudinal vibration, is investigated in [8]. Finding the car-body longitudinal Root Mean Square (RMS) acceleration, from this coupled model, so as to evaluate the ride quality according to ISO standards, is carried out in the present paper.

In the investigation of passenger cars ride quality, it is fundamental to consider all types of inputs which may reduce passenger comfort. Road disturbance, which is applied to each tire and transmitted to the car-body through the corresponding suspension system, is another major vibration input for vehicles. Wong, [2], has given the ISO classification of road unevenness based on the power spectral density and the assumption of a stationary ergodic random process for road profile . A simple quarter-car suspension model has been utilized extensively in the literature since it is suitable to study many essential properties of a real suspension system [9, 10].

This paper assesses the ride quality of a typical rear-drive passenger car with respect to ISO fatigue-decreased proficiency boundaries in vertical and longitudinal directions. The car is equipped with a General Motors (GM) family-II engine. The cylinders' gas pressures have been measured experimentally for three different engine Revolution Per Minute (RPM) and the associated gas and inertia torques are calculated. The driveline and the complete vehicle vibrations, subject to the engine fluctuating torques, are investigated by finding the systems frequency response matrix. Suitable 14-degrees-of-freedom and 18-degrees-of-freedom linear lumped models are employed. The use of system transfer function has two advantages. The first is to straightforwardly obtain damped natural frequencies. The second is to accurately find the driveline forced response since there is no need to guess the initial states, compared to a Runge-kutta numerical procedure. Finally, the vehicle body RMS longitudinal and vertical accelerations are determined and plotted together with the ISO criteria to evaluate the ride quality. The plots support the conclusion that the driveline modes have less effects on the ride quality in comparison with the road excitation, as interpreted by [1].

2. Driveline Torsional Vibration

The driveline is a nonlinear dynamic system that connects the engine to the driving wheels, and it has many modes of vibration. This work studies the driveline torsional vibration and its coupling with longitudinal vibration of the chassis along with their effects on the passenger comfort and vehicle ride quality. A 14-degrees-of-freedom lumped parameter linear model, as seen in Fig. 1, describes the driveline torsional vibration of a rear-drive passenger car equipped with an spark-ignition internal combustion engine. The model consists of different substructures with each substructure including inertia, damping, and stiffness elements which are denoted by J, c, and k, respectively. The nonlinear phenomenons such as backlash, Coulomb friction, and the driveline behavior during clutch engagement, etc., are not included in this study. Further, the rear wheels are fixed to the ground and

it is assumed that the vehicle body mass moment of inertia is large enough. The typical parameters values, for the model under consideration, are given in [7].
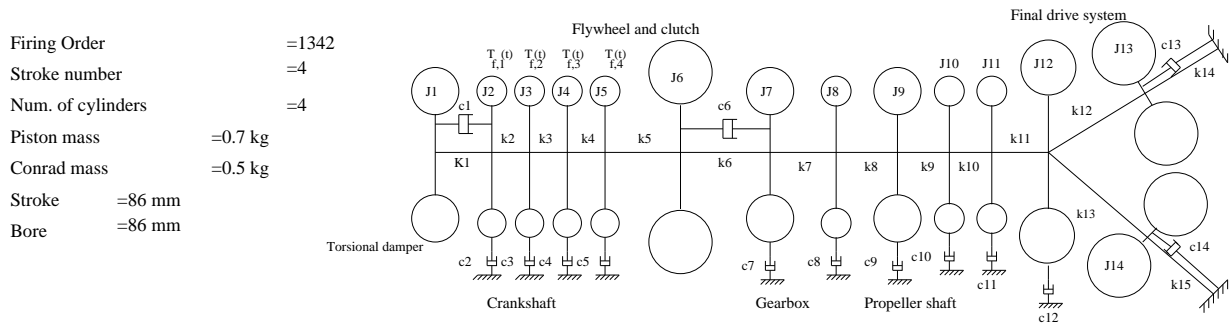
Figure 1. Driveline lumped parameter model.

The applied inputs from the engine (crankshaft) to the driveline are the fluctuating torques, $T_{f,i}(t)$, $i = 1, 2, 3, 4$, of each cylinder. The equations of motion for the vibratory system are

$$\mathbf{M\ddot{x}} + \mathbf{C\dot{x}} + \mathbf{Kx} = \mathbf{F}(t), \quad \mathbf{F}(t) = [0 \ \ T_{f,1}(t) \ \ T_{f,2}(t) \ \ T_{f,3}(t) \ \ T_{f,4}(t) \ \ 0 \ \ \cdots]^T \tag{1}$$

where, $\mathbf{M}$, $\mathbf{C}$, and $\mathbf{K}$ are the mass, damping, and stiffness matrices of sizes 14×14. In addition, $\mathbf{x}$ is a 14×1 vector that involves the rotation of inertia elements. The following subsection is devoted to determining the input vector, $\mathbf{F}(t)$, resulting from the engine.

2.1 Engine Excitation Inputs

2.1.1 Engine Type

A GM Family-II internal combustion engine, is considered here with the characteristics as shown in Fig. 1. Since there is no precise data for all the engine properties, some of the given values are rough estimates of the true values. The gas pressure of one cylinder, during engine operation, is measured experimentally and is shown in Fig. 2. This helps find the corresponding gas torque. Two seconds of measurements are represented. Also, three different engine (crankshaft) speeds of 1000, 2000 and 3000 RPM are considered. The measurement noises have been filtered out in MATLAB.
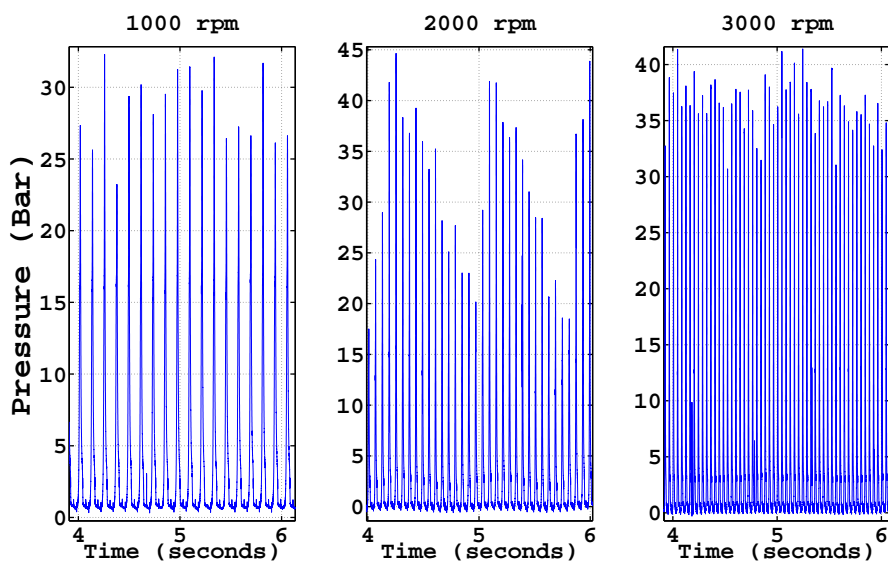
Figure 2. Measured cylinder gas pressure for three different engine speeds.

2.1.2 Engine Mathematical Model

To study the driveline torsional vibration subject to the engine cylinders oscillatory torques, a simulation of the cylinders' rotational dynamics is required. For a four-cylinder engine, four slider-crank mechanisms are applied to model the system. Simplification of each slider-crank mechanism leads to the lumped parameter model consisting of the masses being either in pure rotation or pure translation. According to high stiffness of the compact crankshaft, each cylinder could be finally represented by inertia and stiffness elements, as in Fig. 1, where the total inertia value is the sum of the inertias of the rotating and translatory parts.

2.1.3 Cylinder Total Torque Calculation

The total output torque of cylinder i, i.e., $T_{tot,i}$, is the sum of the gas torque, $T_{g,i}$, and the inertia torque, $T_{inr,i}$. In other words

$$T_{tot,i} = T_{g,i} + T_{inr,i}. \tag{2}$$

The gas pressure torque of each cylinder is approximately determined as [11]

$$T_{g,i} = F_{g,i} r(\sin \omega t + r/l \ \sin \omega t \cos \omega t), \qquad F_{g,i} = P_{g,i} A_p, \ A_P = \pi Bore^2/4. \tag{3}$$

The terms $F_{g,i}$, $P_{g,i}$, A_P, r, ω, t, $Bore$, and $l = 3.5 * r$, are the gas pressure force (N) of the cylinder i, measured pressure (Pa) of cylinder i, piston area (m^2), crank radius (stroke/2) (m), crankshaft angular speed (rad/sec), time (seconds), engine cylinder bore (m), and conrod length (m), respectively. The ratio l/r is a specific characteristic of the engine being equal to 3.5 in this paper. All of the four cylinders' gas pressures are assumed to have the same distribution with a time-shift according to the firing order of the engine, i.e., 1-3-4-2. The power stroke angles are 0, 180, 360, and 540 degrees in every 720 degrees, two revolutions of the crankshaft. The total gas pressure torque of the engine, computed as $T_{g,tot} = \sum_{i=1}^{4} T_{g,i}(t)$, is illustrated in Fig. 3(a) for 720 degrees of crankshaft rotation and different engine speeds. The results show a good agreement with the gas torque of approximately the same engine given by [11].

The inertia torque, produced by each cylinder, is caused by the masses which are in pure translation, i.e., m_r [11]. It is obtained as

$$T_{inr,i} = 1/2 \ m_r r^2 \omega^2 (r/2l \ \sin \omega t - \sin \ 2\omega t \ - 3r/2l \ \sin 3\omega t) \, , \ m_r \approx m_{piston} + 1/3 \ m_{conrod}. \tag{4}$$

The average of the inertia torque is zero and it only adds oscillation to engine total torque, which increases with the engine speed. Substituting Eq. (3) and Eq. (4) in Eq. (2), the total torque of each cylinder, $T_{tot,i}$, is achieved and represented as in Fig. 3(b) for 720 degrees of crankshaft rotation and different engine speeds. While we are interested in the fluctuating part of $T_{tot,i}$, the mean value is computed, as in Fig. 3(b), and it is subtracted from the total torque to only investigate the influences of the cylinders' oscillatory torques as disturbing inputs, i.e., $T_{f,1}(t)$, $T_{f,2}(t)$, $T_{f,3}(t)$, and $T_{f,4}(t)$.

2.2 Driveline Damped Natural Frequencies

In order to find the damped natural frequencies of the driveline, the transfer function matrix of the system, $\mathbf{G}(i\omega)$, is obtained and the desired members of this matrix are plotted in the desired frequency range. It is first required to convert the differential equation of the motion, Eq. (1), to the state space form and further construct $\mathbf{G}(i\omega)$ using this relation. Considering the rotations vector $\mathbf{x}$ and the rotational velocity vector $\dot{\mathbf{x}}$, as the states of the system, the state space form is written as

$$\dot{\mathbf{y}}(t) = \mathbf{A}\mathbf{y}(t) + \mathbf{B}\mathbf{u}(t) \, , \ \mathbf{z}(t) = \mathbf{H}\mathbf{y}(t) \tag{5}$$
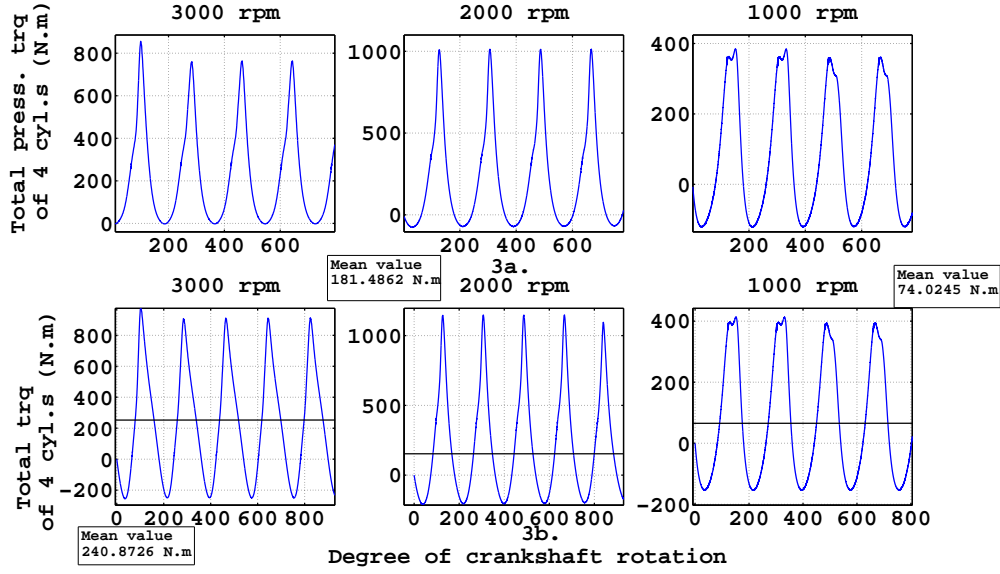
Figure 3. (a) Engine total gas pressure torque, (b) Engine total torque.

where

$$\mathbf{y}_{28\times1} = \begin{bmatrix} \mathbf{x} \ \dot{\mathbf{x}} \end{bmatrix}^T, \mathbf{A}_{28\times28} = \begin{bmatrix} \mathbf{0}_{14\times14} & \mathbf{I}_{14\times14} \\ -\mathbf{M}^{-1}\mathbf{K} & -\mathbf{M}^{-1}\mathbf{C} \end{bmatrix}, \mathbf{B}_{28\times4} = \begin{bmatrix} \mathbf{0}_{14\times4} \\ -\mathbf{M}^{-1}\mathbf{R} \end{bmatrix}, \mathbf{R}_{14\times4} = \begin{bmatrix} 0 & 0 & 0 & 0 \\ & \mathbf{I}_{14\times4} & & \\ 0 & 0 & 0 & 0 \\ \vdots & \vdots & \vdots & \vdots \end{bmatrix} \tag{6}$$

The transfer function matrix in the Laplace domain, is given by $\mathbf{G}(s) = \mathbf{H}(s\mathbf{I} - \mathbf{A})^{-1}\mathbf{B}$ which by exchanging $s = i\omega$ can be transformed to the frequency domain. Fig. 4(a) shows the frequency function between any input applied at point J_2 and the wheel rotation, i.e., state 14, and rotational velocity, i.e., state 28. The five damped natural frequencies that could be excited by input $T_{f,1}(t)$ from the engine are around 3.996, 12.54, 50.76, 109.7, and 138.5 Hz. The lowest natural frequency, i.e., 3.996 Hz, in torsional spectra of the driveline is called shuffle frequency which is usually in the region $2 - 8$ Hz [6]. Investigation of the excitation sources, for this frequency, is of great importance for manufacturers, since human body is more sensitive to vibration in the frequency range $2 - 8$ Hz [1].

2.3 Driveline Forced Response to the Engine Excitation in the Frequency Domain

For a stable driveline system with transfer function $\mathbf{G}(i\omega)$, the Fourier transforms of the outputs which are the states of the system, i.e., $\mathbf{Z}(i\omega)$ in Eq. (5), are

$$\mathbf{Z}(i\omega) = \mathbf{G}(i\omega)\mathbf{U}(i\omega) \tag{7}$$

where $\mathbf{U}(i\omega)$ is the Fourier transform of the input. It is found by employing an appropriate window function, i.e., flattop window in this case, to obtain the accurate estimations of the signal's periodic components. The amplitude spectrum of the Fourier transform of the wheel rotational velocity is shown in Fig. 4(b) for the engine speed of 3000 RPM. For different engine speeds of, e.g., 1000, 2000, and 3000 RPM, there exist different ranges of input excitation frequencies $k \times 8.3$ Hz, $k \times 16.6$ Hz and $k \times 24.9$ Hz, respectively, where $k = 1, 2, ...$ As it was expected, the peaks at 24.9, 49.8, 74.7, and 99.6 Hz in Fig. 4(b), are due to the input force frequencies. It is important to mention that at frequency 50.76 Hz, the system has a natural frequency hence resonance happens and increases the amplitude of vibration.
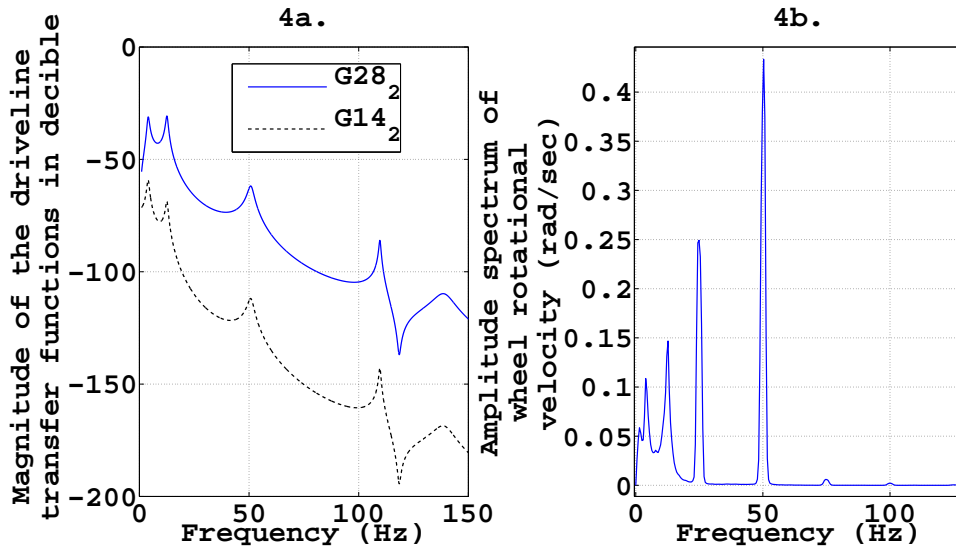
Figure 4. (a) Transfer function of the driveline torsional vibration, (b) The amplitude spectrum of wheel rotational velocity oscillation.

3. Combination of Driveline and Chassis Vibration

The driveline torsional vibration results in torque fluctuation at the driving axle, and therefore, oscillatory drive force will be generated. This finally leads to the longitudinal vibration of the vehicle body. The complete car model, that includes the driveline part and the tire-suspension-body part, is shown in Fig. 5. Here, the parameters values are as in [7]. The connection torque between the two parts, M_a, and the longitudinal force resulting from the Pacejka tire model, F_l, are [7]

$$M_a = k_{12}(\theta_{13} - \theta_{12}) \,, \quad F_l = -A_r(k_{14}z_u + c_{14}\dot{z}_u) - R(k_{13}\theta_t + c_{13}\dot{\theta}_t) \tag{8}$$

where θ, A_r, R, and z_u denote, respectively, the rotation of each element; the coefficient of tire rolling resistance; the typical tire radius in a normal passenger car; and the vertical displacement of unsprung mass (wheel and the associated parts).
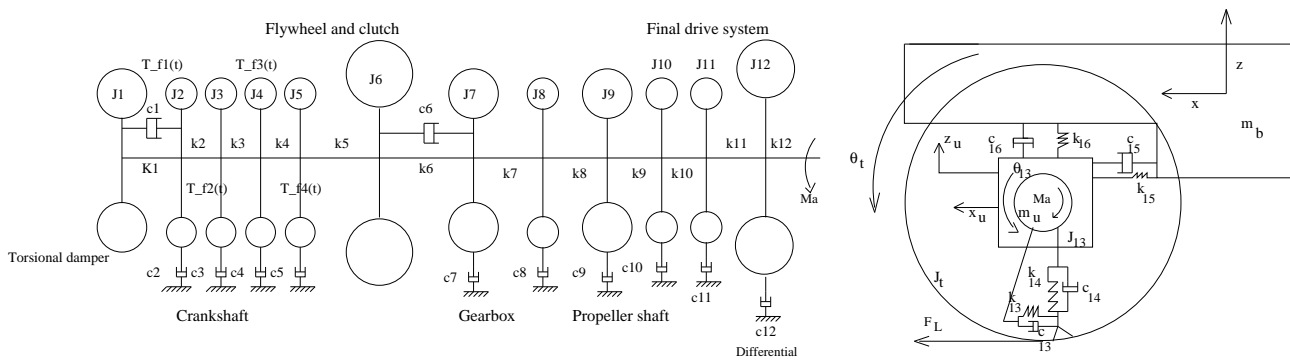
Figure 5. Complete vehicle model.

To study the longitudinal vibration of the vehicle body, m_b, subject to the engine fluctuating torques, the same procedure as in Section 2.3 is used. However, in this case the system has 18-degrees-of-freedom. Obtaining the transfer function of the new system, and substituting it into Eq. (7), the vehicle body longitudinal velocity Fourier transform is computed and shown in Fig. 6, for 3000 RPM of the engine speed. The response has been plotted in dB scale to illustrate the peaks more appropriately. Besides the peaks which result from input excitation frequencies, e.g., 24.9, 49.8, 74.7, and 99.6 Hz, two natural frequencies of the system, 9.25 and 109.85 Hz, are also excited here by the noise in the system input.
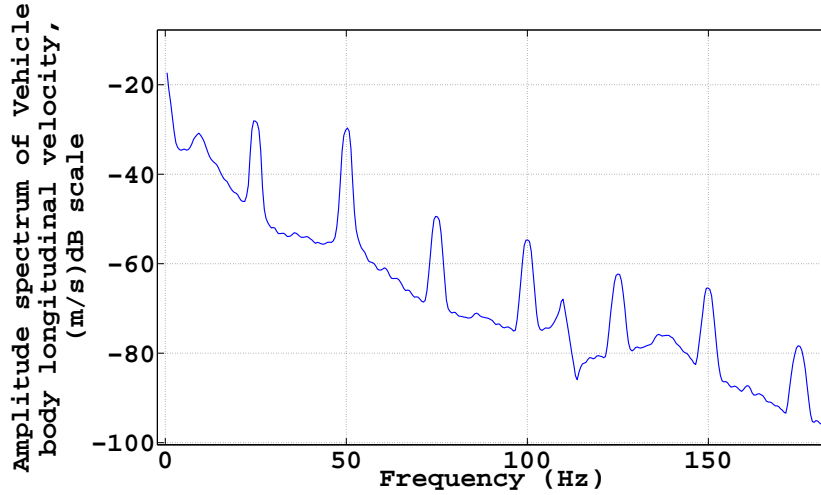
Figure 6. The amplitude spectrum of the body longitudinal velocity oscillation.

4. Vehicle-Body Vertical Acceleration Subject to the Road Excitation

The road surface unevenness results in vehicle-body vertical oscillation which may be experienced by the passengers thereby weakening the ride quality. The suspension system characteristics have the main role to control the amount of this transmission. A linear suspension model with two-degrees-of-freedom, known as the quarter-car model, as in Fig. 7(a), is suitable enough to obtain vertical acceleration of the vehicle-body subject to the road disturbing input [9]. ISO has recommended a stationary random process for modeling the typical road surface profile, which is given in the form of a single sided power spectral density as

$$S_y(f) = \frac{s(n_0)}{v}(\frac{f_0}{f})^2, f \leq f_0 \qquad S_y(f) = \frac{s(n_0)}{v}(\frac{f_0}{f})^{1.5}, f \geq f_0 \qquad (9)$$

Here v is the car constant speed (m/s) with $f_0 = v/2\pi$ and $s(n_0)$ is the degree of roughness which is different for different road classes [2]. The RMS vertical acceleration of the vehicle-body, in a certain frequency f_c, due to the road surface unevenness, $S_y(f)$, which is given in Eq. (9), is determined as

$$\text{Acceleration}_{RMS} = \int_{0.89f_c}^{1.12f_c} S_{\ddot{x}2}(f)\, df, \qquad S_{\ddot{x}2}(f) = \mid H_{\ddot{x}2}(f) \mid^2 S_y(f) \qquad (10)$$

in which, $\mid H_{\ddot{x}2}(f) \mid$ is the transfer function between the input y and the $mass$ 2 acceleration in Fig. 7(a). Also, $S_{\ddot{x}2}(f)$ is the power spectral density of the vehicle-body acceleration.

5. Results and Conclusion

A passenger car is ready for sale when the seat vibration, at the traveling speed of 80 km/hr on a typical inter-urban road, is approximately near to the ISO limitations [1]. Fig. 7(b) shows the RMS accelerations of the vehicle body in longitudinal (dashed line), and vertical (solid line) directions, which are denoted by *body* on the corresponding plots. They are found from the results in Fig. 6 and Eq. (10), respectively. The ISO fatigue-decreased proficiency boundaries during a four-hour exposure time are also represented in Fig. 7(b) in two directions and are pointed by *ISO*. It is assumed that the vehicle is traveling with the mentioned constant speed on an average road roughness with $s(n_0) = 64 \times 10^{-6}$ m^2/cycles/m, [2]. As can be seen, the vehicle-body vertical response subject to the road irregularities is greater than the objective criteria at the frequency region around 1-11 Hz, whereas the longitudinal acceleration, resulting from the engine/driveline modes, is under the ISO

boundary everywhere. This is due to the undamped natural frequencies of the vehicle-body (sprung) and the wheel (unsprung) masses, which are around 2.033 Hz and 11.74 Hz, respectively, using the suspension properties given in Fig. 7(a). Therefore, high excitation frequencies from the engine inputs, which means high value of the frequency ratio, i.e., $\omega_{input}/\omega_{nat,body}$, cause a low transmissibility value [12], and hence a desired vibration isolation for the vehicle-body is achieved. However this will not occur when the system is excited by the low frequency inputs, such as traveling on undulating road, where the transmitted force could be even amplified. Finally, it can be concluded that by using the current passive suspension system, with fixed parameters, it is not possible to reduce the effects of the low frequency disturbances simultaneously with the high frequencies, which is desired from the ride quality aspect.
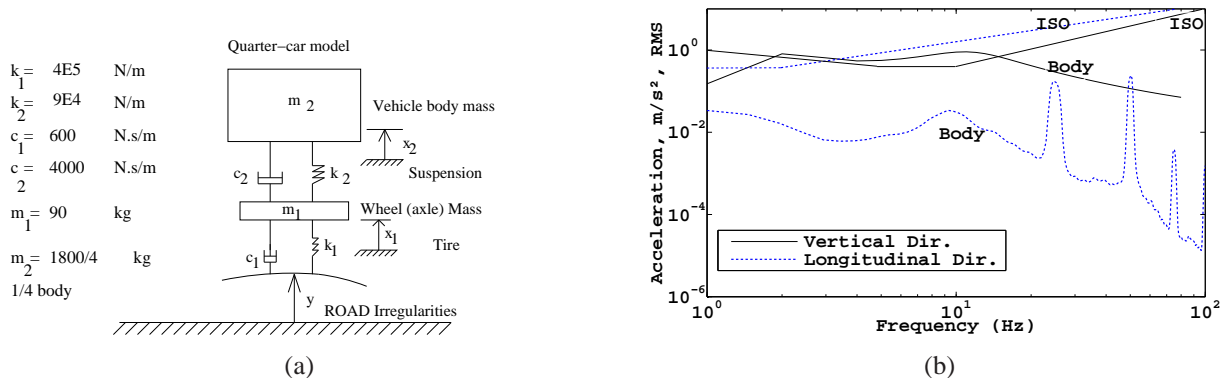
Figure 7. (a) Quarter-car model, (b) Comparison of body RMS accelerations in different directions with ISO criteria.

REFERENCES

[1] Harrison, M., *Vehicle Refinement, Controlling Noise and Vibration in Road Vehicles*, SAE Int., Warrendale, PA 15096-0001 U.S.A., (2004).

[2] Wong, J. Y., *Theory of Ground Vehicles*, John Wiley & Sons, New Jersy, U.S.A., (2008).

[3] Mashhadi, B., and Crolla, D. *Vehicle Powertrain Systems*, John Wiley & Sons, ebook, U.K., (2012).

[4] Crowther, A. R. and Zhang, N. Torsional Finite Elements and Nonlinear Numerical Modelling in Vehicle Powertrain Dynamics, *Journal of Sound and Vibration*, **284** (3-5), 825–849, (2005).

[5] Couderc, Ph., Callenaere, J., Der Hagopian, J. and Ferraris, G. Vehicle Driveline Dynamic Behaviour Experiment and Simulation, *Journal of Sound and Vibration*, **218** (1), 133–157, (1998).

[6] Farshidianfar, A., Rahnejat, H., Ebrahimi, M. and Menday, M. T. Low Frequency Torsional Vibration of Vehicular Driveline Systems in Shuffle, *Multi-body Dynamics: Monitoring and Simulation Techniques (Ed. H. Rahnejat)*, 269–282, (2000).

[7] Rabeih, E., *Torsional Vibration Analysis of Automotive Driveline*, Ph.D. Thesis, Mechanical Engineering Department, The university of Leeds, (1997).

[8] Rabeih, E. and Crolla, D. Coupling of Driveline and Body Vibrations in Trucks, *SAE International*, Technical Paper 962206, (1996).

[9] Turkey, S. and Akcay, H. A Study of Random Vibration Characteristics of the Quarter Car Model, *Journal of Sound and Vibration*, **282** (1-2), 111–124, (2005).

[10] Verros, G., Natsiavas, S. and Papadimitriou, C. Design Optimization of Quarter-car Models with Passive and Semi-active Suspensions under Random Road Excitation, *Journal of Vibration and Control*, **11**, 581–606, (2005).

[11] Norton, R. L, *Design of Machinery*, McGraw-Hill, U.S.A., (1999).

[12] Nickmehr, N., *Ride Quality and Drivability of a Typical Passenger Car subject to Engine/Driveline and Road Non-uniformities Excitations*, Master of Science Thesis, Graduate Program in Mechanical Engineering, Linköping University, (2011).